Influence of Conformational Asymmetry on Polymer−Polymer Interactions: An Entropic or Enthalpic Effect?

Kristoffer Almdal*

The Danish Polymer Centre, Risø National Laboratory, P.O. Box 49, DK-4000 Roskilde, Denmark

Marc A. Hillmyer

Department of Chemistry, University of Minnesota, Minneapolis, Minnesota 55455-0431

Frank S. Bates

Department of Chemical Engineering and Materials Science, University of Minnesota, Minneapolis, Minnesota 55405-0132

Received January 29, 2002; Revised Manuscript Received July 1, 2002

ABSTRACT: The order-to-disorder transition (ODT) of 21 compositionally symmetric diblock copolymers consisting of various combinations of poly(ethylene) (PE), poly(ethyl ethylene) (PEE), poly(ethylene−propylene) (PEP), poly(ethylene oxide) (PEO), and poly(dimethylsiloxane) (PDMS) was used as a measure of the strength of the interaction between the polymers. Conformational asymmetry makes a contribution to polymer−polymer thermodynamics that is not explainable within existing simple theories. For a series of PDMS−hydrocarbon diblock copolymers the observed phase behavior can be rationalized through a self-consistent set of solubility parameters. However, this model as well as other models breaks down when the phase behavior of a series of PEO−hydrocarbon block copolymers is included. We suggest that conformational asymmetry leads to an enthalpic contribution to the Flory−Huggins parameter χ through an effective coordination number which is maximized when both of the blocks have large conformational symmetry parameters, β^2.

1. Introduction

The thermodynamics that govern polymer−polymer mixtures has a controlling influence over a major sector of the commercial plastics and elastomer industries and present some of the most perplexing fundamental problems in modern condensed matter statistical mechanics. Despite more than 50 years of intense study, a unified predictive approach to designing multicomponent polymer alloys with prescribed phase behavior and morphology remains an elusive goal. Nevertheless, during the past few years several new concepts, theoretical approaches, and experimental discoveries have invigorated a productive debate regarding the molecular basis for constructing free energy expressions that account for the subtle variations in mixing entropy and enthalpy that influence miscibility. This publication describes a set of model experiments designed to provide fresh insight into a conceptually simple issue: how variations in local chain structure affect the Flory−Huggins segment−segment interaction parameter.

We reiterate the familiar lattice theory treatment of Flory[1−4] and Huggins,[5,6] which still provides a common framework for characterizing polymer−polymer mixtures. This crude theory separates the mixing free energy (ΔF) of two incompressible melts into two parts that depend on the degree of polymerization N and composition (volume fraction) ϕ,

$$\frac{\Delta F}{k_B T} = \frac{\phi_1}{N_1}\ln \phi_1 + \frac{1-\phi_1}{N_2}\ln(1-\phi_1) + \phi_1(1-\phi_1)\chi \quad (1)$$

The first two terms on the right-hand side of eq 1 are an approximation of the (ideal) combinatorial entropy, and the last term represents the heat of mixing. In its original form the parameter χ captured the energetic penalty associated with breaking pure component segment−segment contacts (ϵ_{11} and ϵ_{22}) and forming cross contacts (ϵ_{12}) in the randomly mixed state,

$$\chi = \frac{z}{k_B T}\left(\epsilon_{12} - \frac{1}{2}(\epsilon_{11} + \epsilon_{22})\right) \quad (2)$$

where z represents the number of such contacts per lattice site. This equation indicates that $\chi \sim T^{-1}$. Normally the form

$$\chi = \frac{A}{T} + B \quad (3)$$

is used. The introduction of the constant B amounts to including an excess entropy term in χ. However, the expansion of eq 2 to eq 3 still ignores many physically important factors like volume changes on mixing and differences in thermal expansivity and compressibility (i.e., equation-of-state effects). Such effects can be empirically accommodated by letting χ (and A and B) be a function of the appropriate parameter and assuming a dependence on the volume fraction of one of the components, Φ, and N is customary.[3] In this paper, we are particularly concerned about the potential effects of differences in packing geometries.

Graessley and co-workers[7−14] have adopted the following approach in explaining their experimental results obtained from more than a dozen model polyolefin mixtures. They ascribe nonideal mixing to classical

* To whom correspondence should be addressed.

10.1021/ma020148y CCC: $22.00
Published on Web 08/17/2002

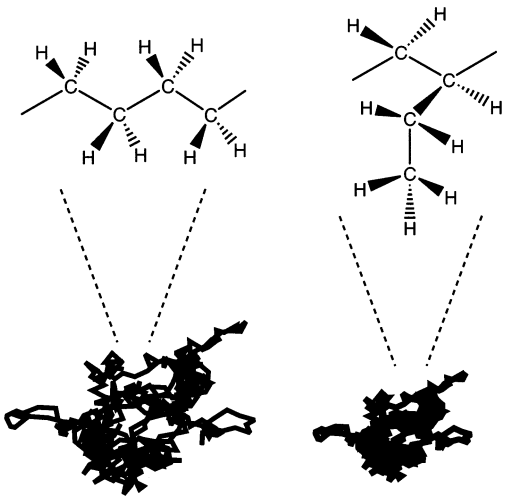

Figure 1. Schematic illustration of the effect of chain statistics on the volume-filling characteristic of a polymer chain. The same random walk (of 500 steps) has been projected to into two-dimensional format by equal volume step where the ratio of the step lengths are given by b_{PE}/b_{PEE}.

differences in pure component solubility parameters,

$$\chi = \frac{v_0}{k_B T}(\delta_1 - \delta_2)^2 \tag{4}$$

where v_0 is the common segment volume and δ is related to the pure component thermal expansivity α and isothermal compressibility, κ_T,

$$\delta = \sqrt{\frac{T\alpha}{\kappa_T}} \tag{5}$$

This approach ignores changes in intra- and interchain structure in the mixed state that may occur due to variations in local crowding. Graessley et al.[14] have been able to correlate their experimental χ values with a self-consistent set of δ parameters for about 75% of their mixtures. Blends that follow this correlation are referred to as regular blends. The remaining irregular blends exhibit anomalous phase behavior. Of particular interest to this work is the empirical linear relation between statistical segment length and δ for polymers in regular mixtures.

We illustrate how simple variation in molecular structure influences polymer conformation and configuration in Figure 1 where we compare two chemical isomers, poly(ethylene) (PE) and poly(ethylethylene) (PEE), which are characterized by a relatively large difference in statistical segment lengths values, b: $b_{PE} \simeq 8.3$ Å while $b_{PEE} \simeq 5.4$ Å at 150 °C.[15−17] The b values are based on a common segment volume v_0 representative of four-carbon repeat units.[18]

On the nonlocal scale—in the limit of large N—the end-to-end distance r_0 is well described in the melt state by Gaussian statistics,

$$R_g^2 = \left\langle \frac{r_0^2}{6} \right\rangle = b^2 \frac{N}{6} = \beta^2 V \tag{6}$$

where $\beta_1^2 = b^2/6v_0$ is the conformational symmetry parameter for the polymer,[16] $V = Nv_0$ is the volume of the polymer, and b is defined by the experimentally determined radius of gyration, R_g, and the degree of polymerization. Note that V is the actual volume per molecule. β^2 describes how far in space the random walk extends per unit volume of polymer chain.

An alternative to the solubility parameter approach that is purely entropic has been offered by Bates and Fredrickson.[19] They argued that the lack of conformational symmetry in athermal polymer blends produces an excess entropy of mixing, $F^E/k_BT = \phi_1(1-\phi_1)\chi_\epsilon$, that results in a positive effective χ parameter[20]

$$\chi_\epsilon \equiv -\frac{1}{2k_BT}\frac{\partial^2 F^E}{\partial \phi_1^2} = \frac{\Lambda_b^3}{24\pi^2 v_0}\left(\frac{1-\epsilon^2}{\phi_1 + (1-\phi_1)\epsilon^2}\right)^2 \tag{7}$$

$\Lambda_b > b$ is a cutoff length that characterizes the nonlocal conformational regime, and the conformational asymmetry is quantified by

$$\epsilon = \frac{\beta_1^2}{\beta_2^2} \tag{8}$$

While eq 7 is qualitatively consistent with certain experimental features (e.g., ϵ dependence of χ in some polyolefin mixtures[17]), the values of Λ_b required to produce the measured magnitude of χ are considerably smaller than the expected limit of Gaussian behavior; for example, $\chi_{PE-PEE} \cong 0.024$ at 150 °C, which implies that $\Lambda_b \cong 6.5$ Å, which is approximately equal to b. This suggests that entropic conformational asymmetry effects may not be primarily responsible for polyolefin immiscibility.[19]

Freed and Dudowicz[21−23] have considered model segment architectures similar to those depicted in Figure 1 in constructing a comprehensive modified lattice theory that accounts for detailed variations in local chain structure. The lattice cluster theory (LCT) uses a different measure of blend structural asymmetry:

$$r \equiv \left|\frac{N_2^{(1)}}{M_1} - \frac{N_2^{(2)}}{M_2}\right| \tag{9}$$

where $N_\alpha^{(i)}$ and M_i are the number of sequentially bonded runs of α bonds and the number united atom groups, e.g., $-CH_2-$, in polymer i, respectively. Both the LCT and conformational asymmetry theories predict a positive excess entropy of mixing and a corresponding reduction in miscibility with increasing structural asymmetry, i.e., $r \neq 0$ and $\epsilon \neq 0$, respectively.

An ambitious theoretical approach has been proposed by Schweizer and Curro[24−28] which addresses the local and nonlocal aspects of nonideal polymer−polymer mixing based on an off-lattice method that relies on the polymer reference interactive site model (PRISM). Unfortunately, this advanced theory does not reduce to simple expressions and does not give an explicit prediction of $(\chi N)_{ODT}$. Although we do not attempt to evaluate the PRISM theory in this paper, our experimental results should be useful in refining this and other advanced theories.

Experiments with model polyolefin mixtures offer certain advantages (e.g., simple segment−segment interactions) in attempting to discriminate between these competing theories. Because these materials form nearly athermal mixtures, the effects of nonidealities created by local structural variations, like short-chain branching, are magnified in the overall free energy balance.

We have exploited both the chemical similarity and structural asymmetries associated with this class of isomers in the work reported here.

Three model polyolefins, PE, PEE, and poly(ethylene−propylene) (PEP), have been combined with two thermodynamically very different polymers, poly(ethylene oxide) (PEO) and poly(dimethylsiloxane) (PDMS), in an attempt to clarify the role of segment structure in polymer−polymer thermodynamics. To simplify the determination of phase behavior, we have worked with a set of symmetric diblock copolymers prepared by anionic polymerization and catalytic hydrogenation.[29] A systematic correlation between the molar mass dependence of the lamellar-to-disorder transition and polyolefin type has emerged, which we interpret as a modification of χ induced by changes in the local segment structure. PEO and PDMS were chosen in order to maximize the interaction energy difference with those polyolefins in the limit of relatively large and small statistical segment length, respectively. In the context of eq 2, this permits us to amplify the effects of variations in local packing, crudely combined into the parameter z, at relatively constant ϵ_{12} where $\epsilon_{11} < \epsilon_{12} < \epsilon_{22}$. This strategy largely avoids the ambiguities associated with interpreting χ parameters when $\epsilon_{11} \approx \epsilon_{12} \approx \epsilon_{22}$ as occur in polyolefin blends.[13,17] Note that both an entropic correction and a z-dependent enthalpic correction to χ will lead to the breakdown of eq 4. The results of this study are discussed in the context of the conformational asymmetry and solubility parameter approaches to dealing with polymer−polymer mixtures.

2. Experimental Section

Sequential anionic polymerization of butadiene or isoprene and of hexamethylcyclotrisiloxane (D_3) was performed in either a hydrocarbon solvent or tetrahydrofuran (THF) with lithium as the counterion. *n*-Hexane or cyclohexane was used for the polymerization of butadiene and isoprene to yield high 1,4-addition. Polymerization of D_3 is facilitated by the addition of hexamethylphosphoric triamide (HMPA) at 0 °C and terminated by addition of a 1.5-fold excess of trimethylchlorosilane. The resulting hydrocarbon−PDMS block copolymers were saturated with deuterium at 35 atm using palladium (5%) on calcium carbonate as a catalyst. Note that high vinyl polybutadienes were synthesized both in hydrocarbon solvent with dipiperidinoethane as chain-end modifier and in THF. The first procedure leads to virtually 100% 1,2-addition of butadiene whereas the use of THF as solvent leads to 90% 1,2-addition. The saturated versions of these polymers are referred to as PEE and PEE90, respectively.

The poly(ethylene oxide) containing block copolymers where synthesized by anionic polymerization of ethylene oxide in THF initiated by a potassium salt of a polymeric alcohol.[30] The molecular details of the materials described in this work are given in Table 1.

Dynamical mechanical measurements in the shear sandwich geometry were conducted using a Rheometrics RSA2 solids analyzer. During the measurements the samples were kept in a temperature-controlled nitrogen atmosphere.

3. Results and Analysis

The order-to-disorder transition temperatures, T_{ODT}, of the 21 diblock copolymers involved in this study where identified by heating the samples at a constant rate while the dynamical mechanical moduli were measured at a constant frequency. This frequency was low compared to the inverse longest relaxation time of the single chain ($\omega \ll 1/\tau$). T_{ODT} is characterized by a large drop in the elastic modulus, G' (see Figures 2 and 3). The T_{ODT} values are given in Table 2.

Table 1

sample	M_n/(kg/mol)[a]	M_n/(kg/mol)[b]	M_w/M_n[c]	f[b,d]	N[a,b,d]
PE−PDMS-1	6.9 ± 0.2	6.8	1.09	0.49	120
PE−PDMS-2	5.9 ± 0.1	6.0	1.14	0.50	102
PEP−PDMS-6	6.4 ± 0.1	6.3	1.07	0.48	106
PEP−PDMS-17	8.6 ± 0.2	7.7	1.13	0.50	148
PEE−PDMS-3	12.7 ± 0.5	10.4	1.07	0.48	214
PEE−PDMS-5	16.8 ± 0.5	15.3	1.07	0.50	289
PE−PEO-1		2.1	1.10	0.48	30
PE−PEO-2		2.8	<1.15	0.48	39
PEO−PEP-1		2.2	1.11	0.52	30
PEO−PEP-2		3.0	1.08	0.51	47
PEO−PEE-12		2.2	1.11	0.52	31
PEO−PEE-2		3.6	1.12	0.48	50

[a] Calculated from stoichiometry. [b] From NMR. [c] From SEC based on polystyrene standards; for PEP−PDMS and PEE−PDMS in THF solution at 30 °C; for PE−PDMS SEC in xylene solution at 100 °C; for PEO containing samples see ref 30. [d] At 413 K assuming no volume change on mixing; $v/m^3 = 8.8 \times 10^{-29} \exp[6.85 \times 10^{-4}(T/K)]$ (=1.168×10^{-28} at 413 K); $\rho_{PDMS} = 0.895$ kg/m^3; $\rho_{PEO} = 1.064$ kg/m^3; for density of hydrocarbons see ref 15.

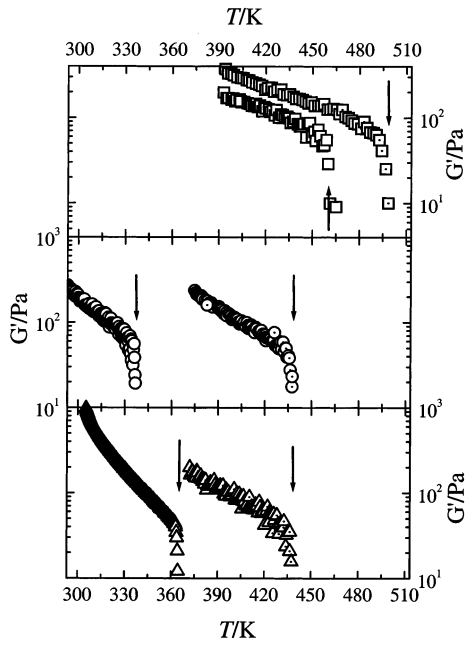

Figure 2. Dynamical mechanical elastic moduli as a function of temperature for PE−PDMS samples (top), PEP−PDMS samples (center), and PEE−PDMS samples (bottom) measured in a shear sandwich geometry. The experimental parameters used for the measurement: the frequency (ω), the strain amplitude (γ_0), and the heating rate (dT/dt) are given in parentheses. PE−PDMS-1 (□; $\omega = 50$ rad/s, $\gamma_0 = 5\%$, $dT/dt = 2$ °C/min), PE−PDMS-2 (⊡; $\omega = 50$ rad/s, $\gamma_0 = 5\%$, $dT/dt = 2$ °C/min), PEP−PDMS-6 (○; $\omega = 10$ rad/s, $\gamma_0 = 5\%$, $dT/dt = 2$ °C/min), PEP−PDMS-17 (○; $\omega = 50$ rad/s, $\gamma_0 = 5\%$, $dT/dt = 1$ °C/min), PEE−PDMS-3 (⊙; $\omega = 10$ rad/s, $\gamma_0 = 5\%$, $dT/dt = 1$ °C/min), PEE−PDMS-5 (dotted △; $\omega = 10$ rad/s, $\gamma_0 = 5\%$, $dT/dt = 2$ °C/min). The arrows indicate the T_{ODT} values determined from the data.

The location of T_{ODT} is uniquely determined by the strength of the interaction, (χN). Thus, by assuming a theory that predicts $(\chi N)_{ODT}$, the value of χ at T_{ODT} can be determined within the framework of the particular theory from $\chi = (\chi N)_{ODT}/N$. Within mean-field theory[31] $(\chi N)_{ODT,\ MF} = 10.495$ for $f = 1/2$, where f is the volume fraction of one of the blocks in the block copolymer. The mean-field theory is expected to be inadequate for the

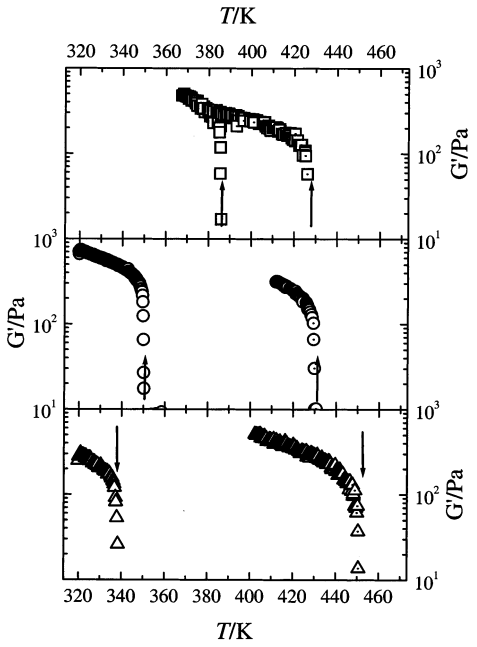

Figure 3. Dynamical mechanical elastic moduli as a function of temperature for PE−PEO samples (top), PEO−PEP samples (center), and PEO−PEE samples (bottom) measured in a shear sandwich geometry. The experimental parameters used for the measurement: the frequency (ω), the strain amplitude (γ_0), and the heating rate (dT/dt) are given in parentheses. PE−PEO-1 (□; $\omega = 1$ rad/s, $\gamma_0 = 1\%$, $dT/dt = 1$ °C/min), PE−PEO-2 (⊡; $\omega = 1$ rad/s, $\gamma_0 = 1\%$, $dT/dt = 1$ °C/min), PEO−PEP-1 (○; $\omega = 1$ rad/s, $\gamma_0 = 2\%$, $dT/dt = 0.5$ °C/min), PEO−PEP-2 (⊙; $\omega = 5$ rad/s, $\gamma_0 = 1\%$, $dT/dt = 1$ °C/min), PEO−PEE-12 (4; $\omega = 1$ rad/s, $\gamma_0 = 1\%$, $dT/dt = 2$ °C/min), PEO−PEE−2 (dotted △; $\omega = 1$ rad/s, $\gamma_0 = 1\%$, $dT/dt = 2$ °C/min). The arrows indicate the T_{ODT} values determined from the data.

Table 2

sample	T_{ODT}/K	b/Å[a]	$10^3\chi_{MF}$[b]	$1000K/T_{ODT}$
PE−PEE-8H	409	7.00	24.6	2.445
PE−PEE-1H	455	6.81	21.6	2.198
PEP−PEE-14	289	6.46	13.5	3.460
PEP−PEE-2	369	6.30	12.0	2.710
PEP−PEE-5	398	6.23	10.9	2.513
PEP−PEE-3	564	5.91	7.37	1.773
PE−PEP-1D	392	7.69	6.67	2.551
PE−PEP-2H	412	7.60	5.47	2.427
PE−PEP-3D	432	7.51	4.58	2.315
PEP−PDMS-6	337	6.20	99.0	2.967
PEP−PDMS-17	438	6.09	70.7	2.283
PE−PDMS-1	498	6.80	87.5	2.008
PE−PDMS-2	458	6.90	103	2.183
PEE90−PDMS-3	383	5.56	49.1	2.611
PEE90−PDMS-5	438	5.65	37.1	2.283
PEO−PEE90-12	337	6.87	338	2.967
PEO−PEE90-2	450	6.85	208	2.222
PE-PEO-1	385	8.10	352	2.597
PE-PEO-2	426	8.00	269	2.347
PEO−PEP-1	350	7.43	351	2.857
PEO−PEP-2	429	7.28	224	2.331

[a] At T_{ODT} calculated from data in ref 15 as the f-weighed geometric mean based on the reference volume defined below Table 1. [b] χ calculation from $(\chi N)_{ODT}$, the functional form $\chi = A/T + B$, and the mean-field (MF) approach.[31]

values of N characterizing the polymers treated in this work. A more complete treatment must include the effect of composition fluctuations. However, simplicity and an earlier experimental analysis[32] provide compelling reasons for using the mean-field approach. Here it suffices to say that the refinement introduced by including fluctuations does not change the qualitative nature of the results.

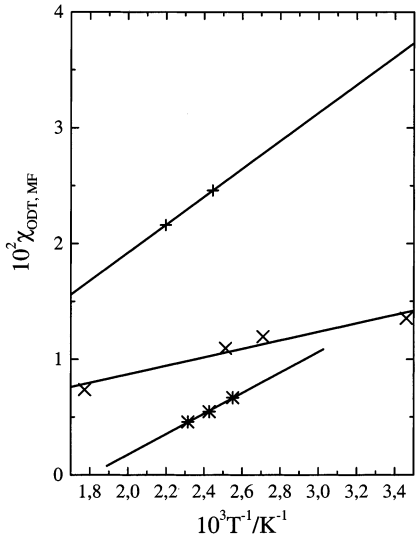

Figure 4. χ_{ODT} (see text) for each of the PE−PEE (+), PEP−PEE (×), and PE−PEP (*) samples. The bold straight lines through the points are fits to eq 3. The parameters are given Table 3.

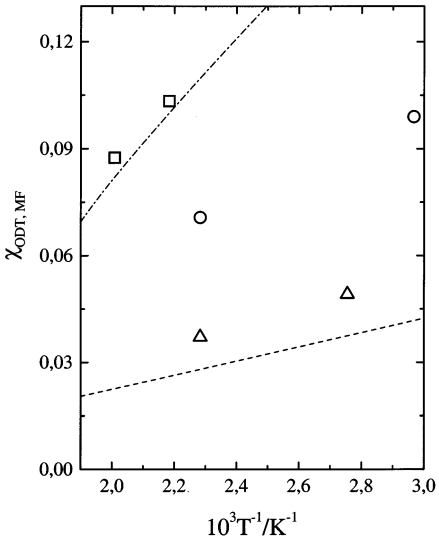

Figure 5. χ_{ODT} (see text) for PDMS containing block copolymers PE−PDMS (○), PEP−PDMS (○), and PEE−PDMS (△). $\chi_{PE-PDMS}$ (− - −) and $\chi_{PEE-PDMS}$ (− − −) according to eq 13.

The experimental χ_{AB} are plotted in Figure 4 for the hydrocarbon block copolymers, in Figure 5 for the PDMS containing block copolymers, and in Figure 6 for the PEO containing block copolymers. Based on the functional form in eq 3, $\chi_{AB}(T)$ is determined for each type of block copolymer. The experimental values of A_{AB} and B_{AB} are given in Table 3.

Based on eq 4 and the experimental $\chi_{AB}(T)$,

$$|\Delta\delta_{AB}(T)| = \sqrt{\chi_{AB}(T)(k_BT/v_0)} \qquad (10)$$

is obtained. The $|\Delta\delta_{AB}(T)|$ for the hydrocarbon diblocks (i.e., PE−PEE, PEP−PEE, and PE−PEP) combined with $|\Delta\delta_{PEP-PDMS}(T)|$ is used to predict $\chi_{PEE-PDMS}(T)$ and $\chi_{PE-PDMS}(T)$. This approach will only fit the experimental data if a self-consistent set of solubility parameters exists for the polymers involved. Thus, for poly-

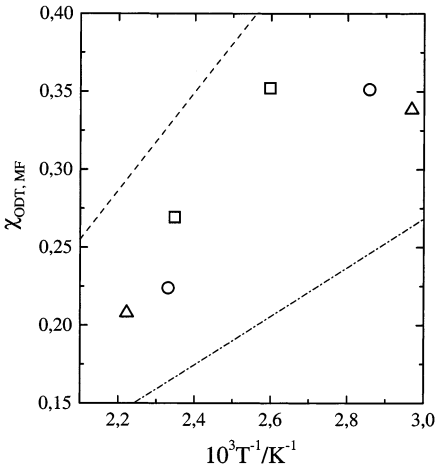

Figure 6. χ_{ODT} (see text) for PEO containing block copolymers PE−PEO (□), PEO−PEP (○), and PEO−PEE (△). The thin lines are the predicted χ_{PE-PEO} (− - −) and $\chi_{PEO-PEE}$ (− − −) according to eq 13.

mers A, B, and C

$$\delta_B(T) = \delta_A(T) + \Delta\delta_{AB}(T) \tag{11}$$

and

$$\Delta\delta_{AC}(T) = \Delta\delta_{AB}(T) - \Delta\delta_{BC}(T) \tag{12}$$

and $\chi_{AC}(T)$ can be written:

$$\chi_{AC}(T) = \frac{v_0}{k_B T}(\Delta\delta_{AC}(T))^2 = \left(\sqrt{\frac{A_{AB}}{T} + B_{AB}} - \sqrt{\frac{A_{BC}}{T} + B_{BC}}\right)^2 \tag{13}$$

Note that the nonzero values of the experimental B_{AB} lead to the slight inconsistency that the predicted χ is nonlinear in $1/T$. This effect is small but visible in Figure 5. The predicted lines are in qualitative and even semiquantitative agreement with the experimental data for PDMS containing block copolymers. For the PEO containing block copolymers the predictions are qualitatively wrong; e.g., the χ parameter is predicted to be smaller in PE−PEO than in PEO−PEP which is opposite to the experimental observations.

Note that all but one of the PEO containing block copolymers used in the present study are methyl-terminated. It is predicted[33] that methylation of the hydroxyl-terminated block copolymer (PEO−PEE90-2) will lower T_{ODT}. Such a change would make the disagreement with the prediction of eq 13 even worse.

The values calculated for $\Delta\delta_{AB}$ using eq 12, listed in Table 3, can be compared with literature values under the assumption that $\delta_{PEO} > \delta_{PE} > \delta_{PEP} > \delta_{PEE90} > \delta_{PEE} > \delta_{PDMS}$; this is justified from the work of Graessley and co-workers.[12] The literature values at 413 K are $10^3\Delta\delta_{PE,PEE90}/\sqrt{Pa} = 1.3$, $10^3\Delta\delta_{PE,PEP}/\sqrt{Pa} = 0.6$, and $10^3\Delta\delta_{PEP,PEE90}/\sqrt{Pa} = 0.7$,[12,34] which compare favorably with the values obtained here, both directly from the hydrocarbon diblock copolymers and from the PDMS hydrocarbon diblock copolymer through eq 12. These $\Delta\delta_{AB}$ values further reinforce the conclusion that for the hydrocarbon polymers and PDMS a self-consistent set of δ_{PE}, δ_{PEP}, δ_{PEE}, and δ_{PDMS} exists which describes the observed phase behavior.

4. Conformational Asymmetry Effects

To facilitate the discussion, we have tabulated the conformational asymmetry parameter ϵ and the LCT r parameter (eq 9)[22] in Table 3. We note that the substantial and negative values of B (negative excess entropy of mixing) are difficult to account for. However, as a note of caution the B values represent extrapolation of the experimental data to $T^{-1} = 0$, which introduces substantial uncertainty. The incompressible LCT theory predicts that the effective excess entropy of mixing $\chi_{eff}^{(S)} \sim r^2$ and can thus not give $B < 0$. The data in Table 3 allow us to arrange the asymmetry parameters according to diminishing ϵ, r, and $\Sigma\beta^2$ where $\Sigma\beta^2 = \beta_A^2 + \beta_B^2$ (see Table 4).

One of the purposes of this study is to clarify the effect of conformational or structural asymmetry on polymer−polymer thermodynamics. Is the effect purely entropically based,[17,19] or is it due to differences in solubility parameters as suggested by Graessley and co-workers[14] based on data obtained from a range of hydrocarbon polymers? The results of the present study indicate that the solubility parameter approach bests explains the polymer−polymer interactions in both PDMS−hydrocarbon and hydrocarbon−hydrocarbon block copolymers consistent with an enthalpically based χ-parameter. Thus, a single set of solubility parameters satisfactorily accounts for the phase behavior of both sets of materials (Figure 5). Conversely, conformational asymmetry theory[19,20] anticipates significantly smaller differences in χ between PDMS and PE, PEP, and PEE than obtained experimentally. Fredrickson et al.[19,20] have speculated that the enthalpic and conformational asymmetry based contributions to χ are additive. Accordingly, $\chi_{A-PDMS} - \chi_{B-PDMS}$ should equal χ_{A-B}, where A and B are saturated hydrocarbon blocks. As indicated in Table 3, this equality fails by a factor of 4−10 at 423 K. The LCT r values have been proposed[22] as a measure of blend structural asymmetry and miscibility. However, the r values are not correlated with χ for either the pure hydrocarbon diblock copolymers or the PDMS containing block copolymers.

For the hydrocarbon−PEO block polymers the solubility parameter approach appears to break down (see Figure 6). The interaction parameters cannot be accounted for using a common set of solubility parameters. The inherent differences in δ_{PE}, δ_{PEP}, and δ_{PEE90} appear to be offset by another effect. We suggest that an enthalpic contribution to the χ parameter that depends on conformational asymmetry, i.e., the β^2 parameter, may be responsible for this effect. Polymers with a large β^2 (see eq 8) offer more contacts with neighboring chains, i.e., lead to a higher effective coordination number, z (eq 2), than those with small β^2. As β^2 is reduced, the fraction of space within a polymer coil conformational volume available to other chains decreases, thereby diminishing z. Accordingly, PEE chains will experience fewer intermolecular segment contacts than equal molar mass PE chains. This variation in z is not accounted for by Flory−Huggins theory (eqs 1 and 2). Based on the solubility parameter relationship alone (eq 4), our data for PDMS, PE, PEP, and PEE anticipate $\chi_{PEO-PEE} > \chi_{PEO-PEP} > \chi_{PEO-PE}$. However, conformational considerations for which $\Sigma\beta^2$ is a qualitative measure yield $z_{PEO-PEE} < z_{PEO-PEP} < z_{PEO-PE}$. We believe these two

Table 3. Conformation Parameters and Fitted Parameters in $\chi = A/T + B$

polymer pair, AB	A	10^3B	$10^3\chi_{423\ K}$	$10^3\lvert\Delta\delta_{AB}\rvert$/Pa$^{1/2}$ [a]	ϵ[b]	r[c]
PE, PEP	8.87	−15.98	4.98	0.5	1.49	0.2
PEP, PEE	3.66	1.37	10.0	0.7	1.59	0.05
PE, PEE	12.1	−4.94	23.6	1.1	2.36	0.25
PEE90, PDMS	25.4	−20.9	39.2	1.4	1.19	0.525
PEP, PDMS	41.4	−23.7	74.0	1.9	1.58	0.55
PE, PDMS	90.7	−94.6	120	2.4	2.36	0.75
PEO, PEP	241.9	−340.0	232	3.4	1.32	0.2
PEO, PEE90	175.1	−181.3	233	3.4	1.75	0.225
PE, PEO	331.5	−508.8	275	3.7	1.13	0

[a] At 423 K from eq 10. [b] $100\beta^2_{PE}/Å^{-1} = 9.67$, $100\beta^2_{PEO}/Å^{-1} = 8.54$, $100\beta^2_{PEP}/Å^{-1} = 6.49$, $100\beta^2_{PEE90}/Å^{-1} = 4.87$, $100\beta^2_{PDMS}/Å^{-1} = 4.11$, and $100\beta^2_{PEE}/Å^{-1} = 4.10$. [c] Infinite molar mass limit. The density difference between the hydrocarbons and PDMS and PEO has been ignored.

Table 4. Different Parameters Arranged in Increasing Order[a]

ϵ_{A-B}	r_{A-B}	$\beta_A^2 + \beta_B^2$
PE−PEE ∼ PE−PDMS	PE−PEO	PEE90−PDMS
PEE90−PDMS	PEP−PEE	PEP−PDMS ∼ PEP−PEE
PEO−PEP	PEO−PEP ∼ PE−PEP	PE−PDMS ∼ PE−PEE
PE−PEP	PEO−PEE90	PEO−PEE90
PEP−PEE ∼ PEP−PDMS	PE−PEE	PEO−PEP
PEO−PEE90	PEE90−PDMS	PE−PEP
PE−PEO	PEP−PDMS	
	PE−PDMS	

[a] The value of the parameter in the header increases from top to bottom of each column. The ∼ symbol indicates approximately equal value of the parameter.

effects largely cancel each other. Here we must emphasize that, although dependent on β^2, this *z effect* is not related to the conformational asymmetry described in refs 19 and 20. In principle, the LCT r value should capture this effect, but the correlation is not obvious.

In a very recent paper Wang has developed a theory for concentration fluctuations in binary blends that explicitly includes differences in conformational asymmetry.[35] The theory can be cast in the form of a fluctuation-renormalized mean-field theory where the *bare* Flory−Huggins parameter, χ^b, is replaced by a renormalized interaction parameter, χ^e, with $\chi^e = \chi^b C + D$. C can be interpreted as an effective normalized coordination number which increases with increasing β^2 values, and D is proportional to the square of the difference between the $1/\beta^2$ values for the two polymers.

For the PDMS−hydrocarbon block copolymers the z effect contribution to χ will operate in concert with the *bare* solubility parameters and will at most lead to inconsistencies in the quantitative interpretation of the ODT results since $\chi_{PEE-PDMS} < \chi_{PEP-PDMS} < \chi_{PE-PDMS}$ and $z_{PEE-PDMS} < z_{PEP-PDMS} < z_{PE-PDMS}$. To verify this hypothesis, more data are needed from block copolymers that contain PE, PEP, and PEE90 and a more complete set of common blocks. Note that most group contribution methods for the calculation of cohesive energies suggest that branching in hydrocarbons, i.e., replacing methylene groups with a combination of methyl and methine groups,[36] reduces the cohesive energy. PE, PEP, and PEE span the range of β^2 and δ available with saturated hydrocarbons, making this set of compounds ideal for evaluating the effects of conformational asymmetry.

5. Conclusions

Conformational asymmetry gives rise to a contribution to polymer−polymer thermodynamics that is not fully explainable within existing simple theories. For a series of PDMS−hydrocarbon block copolymers the observed phase behavior can be rationalized through a self-consistent set of solubility parameters. However, when the phase behavior of a series of PEO−hydrocarbon diblocks is included, the model breaks down. We suggest that conformational asymmetry introduces an enthalpic contribution to the Flory−Huggins χ parameter through an effective coordination number z which is maximized when both components have large conformational symmetry parameters, β^2.

Acknowledgment. This research was supported by the Danish Polymer Center, a Research Center at Risø and at the Danish Technical University sponsored by the Programme for Development of Materials Technology; the United States National Science Foundation through Grant NSF/DMR-9905008.

References and Notes

(1) Flory, P. J. *J. Chem. Phys.* **1941**, *9*, 660−661.
(2) Flory, P. J. *J. Chem. Phys.* **1942**, *10*, 51−61.
(3) Flory, P. J. *Principles of Polymer Chemistry;* Cornell University Press: Ithaca, NY, 1953.
(4) Paul, D. R.; Barlow, J. W.; Keskkula, H. In *Encyclopedia of Polymer Science and Engineering*, 2nd ed.; Mark, H. F., Bikales, N. M., Overberger, C. C., Menges, G., Kroschwitz, J. I., Eds.; John Wiley & Sons: New York, 1988; Vol. 12, pp 399−461.
(5) Huggins, M. L. *J. Chem. Phys.* **1941**, *9*, 440.
(6) Huggins, M. L. *J. Phys. Chem.* **1942**, *46*, 151−159.
(7) Walsh, D. J.; Graessley, W. W.; Datta, S.; Lohse, D. J.; Fetters, L. J. *Macromolecules* **1992**, *25*, 5236−5240.
(8) Balsara, N. P.; Fetters, L. J.; Hadjichristidis, N.; Lohse, D. J.; Han, C. C.; Graessley, W. W.; Krishnamoorti, R. *Macromolecules* **1992**, *25*, 6137−6147.
(9) Graessley, W. W.; Krishnamoorti, R.; Balsara, N. P.; Fetters, L. J.; Lohse, D. J.; Schulz, D. N.; Sissano, J. A. *Macromolecules* **1993**, *26*, 1137−1143.
(10) Balsara, N. P.; Lohse, D. J.; Graessley, W. W.; Krishnamoorti, R. *J. Chem. Phys.* **1994**, *100*, 3905−3910.
(11) Graessley, W. W.; Krishnamoorti, R.; Balsara, N. P.; Fetters, L. J.; Lohse, D. J.; Schulz, D. N.; Sissano, J. A. *Macromolecules* **1994**, *27*, 2574−2579.
(12) Krishnamoorti, R.; Graessley, W. W.; Balsara, N. P.; Lohse, D. J. *Macromolecules* **1994**, *27*, 3073−3081.
(13) Krishnamoorti, R.; Graessley, W. W.; Fetters, L. J.; Garner, R. T.; Lohse, D. J. *Macromolecules* **1995**, *28*, 1252−1259.
(14) Graessley, W. W.; Krishnamoorti, R.; Reichart, G. C.; Balsara, N. P.; Fetters, L. J.; Lohse, D. J. *Macromolecules* **1995**, *28*, 1260−1270.
(15) Fetters, L. J.; Lohse, D. J.; Richter, D.; Witten, T. A.; Zirkel, A. *Macromolecules* **1994**, *27*, 4639−4647.
(16) Bates, F. S.; Schultz, M. F.; Khandpur, A. K.; Förster, S.; Rosedale, J. H.; Almdal, K.; Mortensen, K. *Faraday Discuss. Chem. Soc.* **1994**, *98*, 7−18.

(17) Bates, F. S.; Schulz, M. F.; Rosedale, J. H.; Almdal, K. *Macromolecules* **1992**, *25*, 5547−5550.
(18) Rosedale, J. H.; Bates, F. S.; Almdal, K.; Mortensen, K.; Wignall, G. D. *Macromolecules* **1995**, *28*, 1429−1443.
(19) Bates, F. S.; Fredrickson, G. H. *Macromolecules* **1994**, *27*, 1065−1067.
(20) Fredrickson, G. H.; Liu, A. J.; Bates, F. S. *Macromolecules* **1994**, *27*, 2503−2511.
(21) Dudowicz, J.; Freed, K. F. *Macromolecules* **1995**, *28*, 6625−6641.
(22) Freed, K. F.; Dudowicz, J. *Macromolecules* **1996**, *29*, 625−636.
(23) Freed, K. F.; Dudowicz, J. *Macromolecules* **1998**, *31*, 6681−6690.
(24) Singh, C.; Schweizer, K. S. *J. Chem. Phys.* **1997**, *103*, 5814−5832.
(25) Schweizer, K. S.; Singh, C. *Macromolecules* **1995**, *28*, 2063−2080.
(26) David, E. F.; Schweizer, K. S. *Macromolecules* **1997**, *30*, 5118−5132.
(27) Guenza, M.; Schweizer, K. S. *J. Chem. Phys.* **1997**, *106*, 7391−7410.
(28) Singh, C.; Schweizer, K. S. *Macromolecules* **1997**, *30*, 1490−1508.
(29) Ndoni, S.; Papadakis, C. M.; Bates, F. S.; Almdal, K. *Rev. Sci. Instrum.* **1995**, *66*, 1090−1095.
(30) Hillmyer, M. A.; Bates, F. S. *Macromolecules* **1996**, *29*, 6994−7002.
(31) Leibler, L. *Macromolecules* **1980**, *13*, 1602−1617.
(32) Maurer, W. W.; Bates, F. S.; Lodge, T. P.; Almdal, K.; Mortensen, K.; Fredrickson, G. H. *J. Chem. Phys.* **1998**, *108*, 2989−3000. It is well-established that χ parameters determined for block copolymers are related to the associated binary homopolymer bland interactions parameters, $\chi_{A/B}$, generally measured by small-angle neutron scattering (SANS). However, as described in an earlier publication, there are four different ways to determine χ with block copolymers: using disordered state (correlation hole) SANS (or SAXS) data, or based on T_{ODT}, with a mean-field or fluctuation treatment possible in each case. A comprehensive analysis of PE−PEP diblock copolymers and the corresponding PE/PEP homopolymer blend revealed near exact agreement between $\chi_{A/B}$ and $(\chi N)_{ODT,\ MF}$. On the basis of this result, we have chosen to use the mean-field treatment for the determination if χ. For simplicity, we refer to these interaction parameters as χ_{AB} in the remainder of this report.
(33) Frielinghaus, H.; Pedersen, W. B.; Larsen, P. S.; Almdal, K.; Mortensen, K. *Macromolecules* **2001**, *34*, 1096−1104.
(34) Graessley, W. W.; Krishnamoorti, R.; Balsara, N. P.; Butera, R. J.; Fetters, L. J.; Lohse, D. J.; Schulz, D. N.; Sissano, J. A. *Macromolecules* **1994**, *27*, 3896−3901.
(35) Wang, Z.-G. *J. Chem. Phys.* **2002**, *117*, 481−500.
(36) Krevelen, D. W. V. *Properties of Polymers. Their Correlation with Chemical structure; Their Numerical Estimation and Predicition From Additive Group Contributions*, 3rd ed.; Elsevier: Amsterdam, 1990.

MA020148Y